JOURNAL OF CATALYSIS 136, 24–42 (1992)

Model Studies of Cesium Promoters in Water–Gas Shift Catalysts: Cs/Cu(110)

J. M. CAMPBELL, JUNJI NAKAMURA, AND CHARLES T. CAMPBELL

Department of Chemistry, University of Washington, BG-10, Seattle, Washington 98195

Received September 20, 1991; revised January 31, 1992

The kinetics and the mechanism of the water–gas shift (WGS) reaction have been studied over a Cu(110) surface containing vapor-deposited Cs adatoms. The optimum rate occurs for a Cs coverage of about one cesium atom per four Cu surface atoms. Postreaction surface analysis (XPS, AES, TDS) proves that this Cs is almost immediately converted to a surface complex containing cesium, oxygen, and carbon under reaction conditions. This complex has TDS, XPS, and AES features similar to a surface cesium carbonate, $C_{s_x} \cdot CO_{3,a}$ (x = 1.5 to 2.0). The kinetics of the elementary reaction steps leading to the formation and decomposition of this carbonate are also studied. These steps are in rapid equilibrium under reaction conditions. The electronic effects of the Cs_a on the elementary steps of the WGS reaction are also investigated. Cesium causes an acceleration in water dissociation on the surface and in the conversion of surface oxygen to CO_2 by CO. The former reaction is rate-limiting with no Cs present, whereas the latter partially controls the rate on the optimally promoted surface.

I. INTRODUCTION

Alkali metals are known to promote many catalytic reactions (*1*). In particular, cesium accelerates the water–gas shift (WGS) reaction, $H_2O + CO \rightarrow H_2 + CO_2$, and methanol synthesis over Cu-based catalysts (*1–8*). The water–gas shift reaction over Cu catalysts has been the subject of considerable study (*3, 7–16*). In such catalysts, metallic Cu is the active site for WGS in the absence of Cs (*8–10*). The (111) single-crystal face of pure copper also shows a significant rate enhancement with the addition of small coverages of cesium (*7*). For example, a coverage of $\Theta_{Cs} = 0.13$ on Cu(111) increases the WGS rate at 612 K to approximately 15 times that of the clean Cu(111) surface. For these reasons, studies of Cs on Cu single-crystal surfaces serve as a good model for Cs promotional effects on more practical Cu-based catalysts.

The mechanism and kinetics of WGS over clean Cu(110) have been discussed previously (*8*), where the "surface redox" or "oxygen adatom" mechanism was used to explain the results. In this mechanism, H_2O dissociates completely to an oxygen adatom (O_a) and H_2 (via $2H_a$), and the O_a is then titrated by CO (*3, 7–16*). (Here, the subscript "a" refers to an adsorbed species.) The rate-determining step (RDS) for WGS over clean Cu(110) was determined to be the initial dissociation of H_2O, $H_2O \rightarrow H_a + OH_a$ (*8*). A full energetic and mechanistic model for this reaction on clean Cu(110) has been presented previously (*8, 17*).

Kinetic measurements of the WGS reaction on the Cs-promoted Cu(111) surface have been reported in an earlier study (*7*). The increase in activity is obviously due to an acceleration of the rate-determining step, which is dissociative water adsorption (*7*). However, a great deal concerning the form of the Cs promoter on the working catalyst and the effects of this promoter on the various elementary steps is still unclear. In this paper, we address these issues by studying the kinetics and mechanism of the WGS reaction and its elementary steps over the Cu(110) surface containing various coverages of vapor-deposited cesium. The sur-

0021-9517/92 $5.00

face species existing during WGS over Cs/Cu(110) are also examined here with postreaction TDS, XPS, and AES. The Cu(110) surface was chosen for this study because this plane is the best understood with respect to the mechanism of WGS on clean Cu (without Cs_a). Also, the kinetics could be compared to previous kinetics for the Cs-promoted Cu(111) surface to assess the structural sensitivity of the Cs promotional effect.

As we show, the cesium appears to exist on the working catalyst mainly in the form of a surface carbonate, $Cs_x \cdot CO_{3,a}$, with x taking values between $\frac{1}{2}$ and 1, although other forms of the cesium are also present in small quantities, the concentrations of which are determined by equilibrium reactions with gaseous reactants and products. Interestingly, surface carbonate species are never seen on the Cu(110) surface in the absence of Cs (*25*). To determine the role of this cesium carbonate species in the WGS, experiments involving carbonate formation and reactions of the carbonate decomposition product, $Cs \cdot O_a$, were also performed.

There also exist extensive prior data concerning elementary interactions of CO (*18–25*), CO_2 (*25, 26*), H_2O (*27–31*), and H_2 (*32–38*) with Cu(110) and with Cs/Cu(110). Most important among those prior results with regard to the present paper are the following conclusions. (1) Low coverages of Cs ($\Theta_{Cs} \leq 0.25$) stabilize CO_a by up to 15% compared to clean Cu(110). At coverages beyond the work-function minimum ($\Theta_{Cs} > 0.25$), a surface $Cs \cdot CO_a$ complex, which is even more stable, is produced (*25*). (2) At 110 K, CO_2 reacts rapidly with low-coverage Cs_a in UHV to produce some species that convert to a surface Cs carbonate by 300 K via the reaction $Cs_a + 2CO_2 \rightarrow Cs \cdot CO_{3,a} + CO$. This carbonate decomposes at ~550 K to liberate CO_2 gas and leave $Cs \cdot O_a$ on the surface (*25*). Here, $Cs \cdot O_a$ refers to coadsorbed Cs and oxygen adatoms, which are each bonded mainly to Cu but which probably have some direct Cs–O bonding (or at least they strongly mutually stabilize each other). This $Cs \cdot O_a$ can also be produced by dosing O_2 to Cs_a (*30*). (3) Adsorbed H_2O is stabilized by both Cs_a and $Cs \cdot O_a$. Also, H_2O will readily react with high Cs coverages ($\Theta_{Cs} \geq 0.32$) to produce $Cs \cdot OH_a$ and H_a. This H_a is stabilized by Cs_a and $Cs \cdot OH_a$, since it desorbs as H_2 gas only at ~430 K, compared to 320–340 K in the absence of Cs (*30*). (4) Adsorbed oxygen (O_a) and $Cs \cdot O_a$ are readily reduced by H_2 (via $2H_a$) to produce water, occurring with reaction probabilities of $\sim 4 \times 10^{-6}$ and $\sim 8 \times 10^{-7}$, respectively, at 573 K (*37, 38*). On the basis of these data, we discuss here the kinetics and mechanism of the WGS reaction over Cs-promoted Cu(110). These results have been briefly presented in a preliminary report (*8*).

II. EXPERIMENTAL

The apparatus and the procedures used in this study are described elsewhere (*8, 25*). The apparatus consists of a medium pressure batch microreactor for measuring catalytic reactions, which allows us to introduce high pressures (up to ~2 atm) of reactants and a UHV chamber (base pressure $< 10^{-10}$ Torr) for surface analysis with capability for TDS, XPS, AES, $\Delta\phi$, LEED, and Ar^+ sputter cleaning. The sample can be rapidly transferred (<20 s) between these chambers without exposure to air or other gases. The sample was resistively heated by Ta wires passing through grooves on the sides of the single-crystal sample.

The coverages (Θ) reported here are given relative to the Cu(110) surface atom density of 1.085×10^{15} atoms $\cdot$ cm^{-2}. Absolute coverages were determined using the AES peak-to-peak ratios and XPS peak area ratios calibrated previously for this instrument (*25, 31*). The O (KVV)/Cu (LVV) AES ratio of 0.085 and the O (1*s*)/Cu ($2p_{3/2}$) XPS ratio of 6.2×10^{-3} were assigned to a surface oxygen coverage of $\Theta_O = 0.5$ (*25, 31*). The O (KVV)/Cu(LVV) AES ratio was used for coverage calibration only for oxygen adatoms. The surface carbonate produced O (KVV) spectra with drastically different

lineshapes (see Results), so the peak-to-peak ratios proved unreliable for oxygen coverage estimation. The carbonate coverages were, therefore, determined by O (1*s*) and C (1*s*) XPS. The Cs (560 eV)/Cu (920 eV) AES ratio of 0.08 and the Cs($3d_{5/2}$)/Cu ($2p_{3/2}$) XPS ratio of 0.13 were previously assigned to the closest-packed monolayer of Cs on Cu(110) (*25*), which corresponds to a cesium coverage of $\Theta_{Cs} = 0.48$ (*39*). The Cs coverages except where noted were usually determined by AES taken prior to reaction. The presence of adsorbed oxygen or of other anions changes the AES lineshape in the Cs region, resulting in a large increase (up to 50%) in the intensity of the Cs peak-to-peak signal, as seen previously (*25, 31*). Although the Cs coverages could be estimated from postreaction AES measurements with appropriate consideration of this effect, the prereaction AES measurements of Cs coverage were more precise and more reliable, and they were therefore generally used to assess Cs coverage. Control experiments using quantitative XPS measurements taken before and after WGS reactions showed that very little Cs was lost during the reaction at the Cs coverages ($\Theta_{Cs} \leq 0.3$) and at the reaction temperatures ($T \leq 573$ K) of most interest here.

We briefly studied the adsorption of Cs on Cu(110) with ion scattering spectroscopy (ISS) using 1.3-kV He^+ ions, incident 60° from normal, and detection normal to the surface. The Cu signal decreased rapidly to nearly zero at the work function minimum, which corresponds to only about one-half of a close-packed monolayer of cesium (*25*). This rapid decrease is thought to be due to a combination of the usual masking effects due to Cs atoms and a greatly increased He^+ neutralization probability due to the work function decrease caused by Cs_a (*40*). Consistent with this is the fact that the slope of the Cs ISS signal versus Cs coverage decreased strongly in the first one-half monolayer, was zero around one-half monolayer ($\Theta_{Cs} = 0.24$), and increased again at higher coverage.

For the WGS reactions studied here, CO and H_2O pressures of 26 and 10 Torr, respectively, were used except where noted. Because of condensation on walls, no H_2O pressures above 18 Torr were used. A total of 1000 Torr of N_2 was also added to the reactants because its flow into the differential pumping stages during sample transfer from the microreactor back into UHV eliminated impurity buildup during transfer. It was proven to have no effect on the reaction rates.

III. RESULTS

1. *Kinetics of WGS on Cs/Cu(110) at Low Conversions*

a. Review of kinetic results. Plots of the steady-state rate of WGS over Cu(110) as a function of Cs coverage for reaction temperatures between 473 and 573 K were reported in our preliminary communication of these results (*8*), but they are briefly summarized again here. The WGS reactions were performed at low conversions in a microreactor typically using 10 Torr H_2O and 26 Torr CO over a heated Cs/Cu(110) surface. The reaction was always run long enough to ensure steady-state rates and the production of many hundreds of product molecules per surface Cu atom (*8*). The addition of Cs to the Cu(110) surface promoted the rate of WGS up to a maximum fivefold enhancement at the optimum Cs coverage, $\Theta_{Cs} = 0.25$. With higher cesium coverages (up to $\Theta_{Cs} = 0.55$), the WGS rate decreased from this optimum condition, but remained higher than the WGS rate over clean Cu(110). The apparent activation energy of WGS on optimally promoted ($\Theta_{Cs} \approx 0.25$) Cs/Cu(110) was 11 kcal/mol, compared to 10 kcal/mol for WGS over the clean Cu(110) surface. Near our typical reaction conditions at 523 K, the WGS reaction over Cs/Cu(110) was shown to be approximately half-order in CO pressure and about zero-order in H_2O pressure (*8*). Above ~100 Torr of CO, however, the dependence on CO pressure approached zero-order, while the H_2O pressure dependence became half- to

first-order. On the clean Cu(110) surface, the order in H_2O pressure was 0.9 ± 0.2 and the order in CO pressure was 0.2 ± 0.2 over all pressures examined (*8*).

Because we are interested in the promotional effect of Cs, which is a maximum at $\Theta_{Cs} = 0.25$, most of the TDS, XPS, and AES experiments presented in the following were obtained at $0.18 \leq \Theta_{Cs} \leq 0.27$, i.e., near the optimum coverage, unless otherwise stated.

b. Influence of CO_2 on the rate of WGS on Cs/Cu(110). The rate of the WGS reaction was also measured over Cs-promoted Cu(110) with the addition of product CO_2 to the reactant mixture. When 10 Torr CO_2 was added to the reaction mixture of 10 Torr H_2O and 26 Torr CO, the WGS rate at 523 K and $\Theta_{Cs} \approx 0.25$ was reduced by a factor of 2 compared to the WGS rate at the same Cs coverage without the addition of CO_2 to the reaction mixture. In the latter case, CO_2 is produced, but for our reaction times the CO_2 pressure was only ~1 Torr at the end of the reaction. It should be noted that even with 10 Torr of added CO_2, the reaction was still far from equilibrium throughout the time the reaction was run. Using the WGS equilibrium constant at 523 K reported by Newsome (*11*), $K_p = 84$, the equilibrium pressure of CO_2 under these conditions (with CO_2 preaddition) would be 20 Torr. Also, the H_2 pressure produced during this reaction was still a factor of 10 below its equilibrium value. Thus, this deceleration of rate due to CO_2 addition is probably not due to competition from the reverse reaction, but instead must be associated with some CO_2 effect on the surface conditions.

2. Postreaction Surface Analysis

Figure 1a shows the CO_2 and Cs TDS from typical postreaction surfaces (low conversion) at various Cs coverages. To obtain these spectra, the clean Cu(110) sample was first predosed with Cs, transferred to the microreactor, pressurized with 16 Torr H_2O, 42 Torr CO, and ~1000 Torr N_2, and then heated to the reaction temperature of 473 K. After establishing steady-state WGS kinetics (~3 min) at 473 K, the current for heating the sample was turned off and the sample was immediately transferred from the reactor to UHV while cooling. Below $\Theta_{Cs} = 0.25$, a single CO_2 TDS peak was observed in postreaction analysis, with a constant peak temperature of 530 K. However, above $\Theta_{Cs} = 0.25$, an additional shoulder appeared at a higher temperature (~560 K), which shifted to still higher temperatures with increasing Cs coverage. It should be noted that no adsorbed species nor CO_2 desorption was observed after WGS over clean Cu(110) without Cs_a (*8*) and CO_2 has a negligible coverage on clean Cu(110) at these reaction temperatures and product CO_2 pressures (*25, 26*). Cesium desorption peaks ($m/e = 133$) were observed at 630 and 680 K with a minor peak at 550 K (Fig. 1a). No other desorption products were detected during TDS of the postreaction surface; however, desorption of small amounts of H_2 and H_2O might not have been observable because of the high background pressure (10^{-9}–10^{-8} Torr) consisting primarily of water, with some H_2, brought into the analysis chamber by the transfer rod and sample holder.

The postreaction TDS of Fig. 1a are similar in several respects to those reported in a previous UHV study of the interaction of 2.3 Langmuir (L) CO_2 with Cs/Cu(110) at 110 K (*25*). Because the interpretation of those results are pertinent to our analysis of the post-WGS surface, they are reproduced in Fig. 1b (*25*). The desorption of CO_2 above ~500 K in these spectra was shown previously to be due to the decomposition of a surface carbonate complex intimately associated with the adsorbed cesium, $Cs \cdot CO_{3,a}$, which was formed from dosing CO_2 to a cesium-covered Cu(110) surface (*25*). The $Cs \cdot CO_{3,a}$ complex was formed via

$$2CO_2 + Cs_a \rightarrow Cs \cdot CO_{3,a} + CO, \quad \text{(I)}$$

at surface temperatures as low as ~180 K, and decomposed upon heating via

$$Cs \cdot CO_{3,a} \rightarrow Cs \cdot O_a + CO_2. \quad \text{(-II)}$$

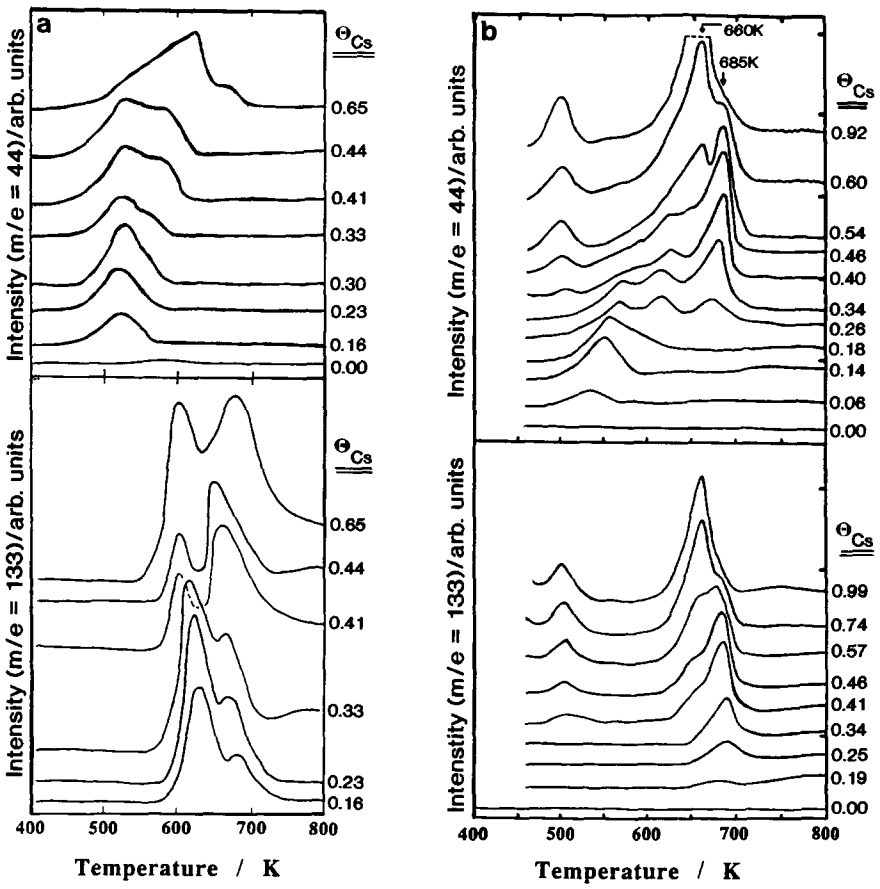

FIG. 1. TDS spectra for CO_2 (m/e = 44) and for Cs (m/e = 133) with different Cs precoverages: (a) After steady-state WGS reaction kinetics at 16 Torr H_2O, 42 Torr CO, ~1000 Torr N_2, and 473 K. (b) After dosing 2.3 L CO_2 to Cu(110) at ~110 K (from Ref. (*25*)).

The thermal desorption of pure Cs on Cu(110) occurs below 500 K for Cs coverages in excess of 0.25 (*25*), whereas the $Cs \cdot CO_{3,a}$ is stable to 600–700 K, which proves that adsorbed cesium is stabilized by the carbonate (*25*). Of course, the surface oxygen remaining after carbonate decomposition also stabilizes the surface cesium (*25, 30*).

The CO_2 desorption peak in Fig. 1b at 530–560 K (*25*) for cesium coverages below 0.25, which is due to $Cs \cdot CO_{3,a}$ decomposition (*25*), is very similar to the CO_2 desorption peak at 530 K observed in Fig. 1a after WGS reaction for $\Theta_{Cs} \leq 0.25$. This suggests that this CO_2 peak is also due to the decomposition of surface cesium carbonate. In contrast, formate coadsorbed with cesium on Cu(110) decomposes already at a much lower temperature, giving a sharp CO_2 TDS peak at 425–460 K accompanied by H_2 (*50*). This difference in CO_2 TDS peak temperature and the absence of any observable H_2 peak rule out formate decomposition as a source of this postreaction CO_2 TDS peak. Postreaction XPS and AES data also support an assignment of surface cesium carbonate at $\Theta_{Cs} = 0.20$ (see below). The postreaction Cs TDS spectra for $\Theta_{Cs} \leq 0.25$ are substantially different in lineshape after reaction compared to that after simply dosing CO_2 to Cs_a at 110 K. However, the general

temperature range of Cs desorption is quite similar (~600–700 K compared to ~650–700 K). This Cs desorption temperature is of course controlled by the interaction strength of Cs with the surface oxygen remaining on the surface *after* carbonate decomposition (*25, 30*) and is much higher than the peak temperature of ~510 K associated with the decomposition of $Cs \cdot OH_a$ (*30*) or formate coadsorbed with Cs on Cu(110) (*50*). The Cs lineshape differences for $\Theta_{Cs} \leq 0.25$ in Fig. 1a versus 1b may be due to small amounts of minority species also present on the surface after reaction or to different coverages or distributions of surface oxygen achieved in the postreaction surface.

There are also marked lineshape differences between Figs. 1a and 1b for Θ_{Cs} above 0.25. Nevertheless, some similarities are also obvious: (1) desorption of CO_2 occurs in roughly the same temperature range (500–700 K); (2) the CO_2 desorption peaks generally show a filling in of higher temperature states as the Cs coverage increases; (3) desorption of Cs occurs in roughly the same temperature range (580–720 K versus 630–700 K); and (4) the Cs desorption peaks generally shift to lower temperature with increasing coverage. Of course, any TDS peaks in Fig. 1b below ~510 K will not be seen in the postreaction spectra of Fig. 1a since the surface of Fig. 1a was maintained at 473 K during reaction and was evacuated at ~460–450 K while cooling. Because of these similarities, we assign the post-WGS reaction species (Fig. 1a) to some type of surface cesium carbonate complex similar to that of Fig. 1b.

The CO_2 TDS peak areas from the postreaction surface such as presented in Fig. 1a increased linearly with cesium coverage as shown in Fig. 2, suggesting that every Cs atom on the surface was associated with a CO_3 ion or ions in a fixed stoichiometric ratio. Quantitative XPS (below) shows the CO_3 : Cs ratio to correspond to 1.5, whereas this ratio was 1 for the UHV-dosed CO_2 corresponding to Fig. 1b (*25*), which may explain some of the differences in the TDS lineshapes.

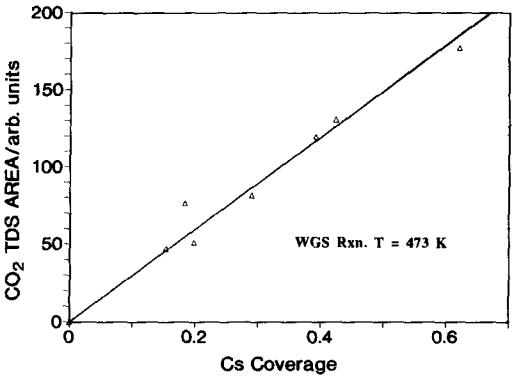

FIG. 2. Integrated TDS areas of CO_2 peaks observed in postreaction TDS as a function of Cs coverage. The conditions here are the same as those described in Fig. 1a.

The reaction temperature had little effect on the postreaction CO_2 and Cs TDS lineshapes for Cs coverages of ~0.2 but only caused a decrease in the integrated CO_2 TDS area with increasing reaction temperature, due to the removal of intensity from the lower-temperature part of the spectrum. The steady-state coverage of the surface carbonate should decrease as the reaction temperature approaches the carbonate decomposition temperature; therefore, a reduction in the CO_2 TDS area with reaction temperature was expected. At reaction temperatures much above the CO_2 desorption peak temperature of 530 K for $\Theta_{Cs} \approx 0.2$, very little CO_2 evolution was observed in TDS of the post-WGS surface.

Surface analysis was also performed after WGS, but where the surface was cooled to ~373 K in the reaction mixture. In this way, surface species likely to desorb at reaction temperature during evacuation will be retained. In Fig. 3, a post-WGS CO_2 TDS spectrum when the Cs/Cu(110) surface was cooled in the reactor is compared to a similar spectrum of a surface that was cooled during transfer to UHV. In both cases the WGS reaction preceding the TDS was performed with a Cs coverage of ~0.27 under the same

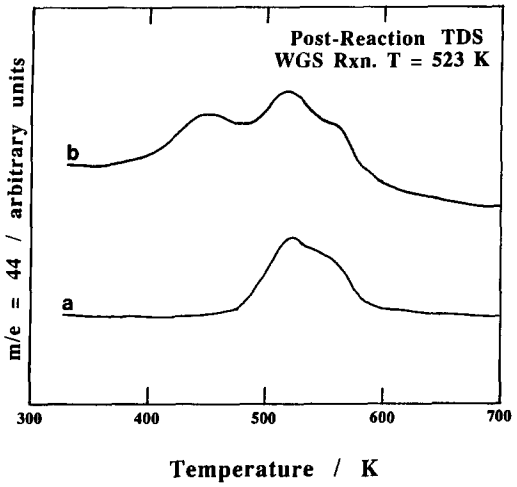

FIG. 3. Comparison of postreaction CO_2 TDS after different transfer procedures: (a) The sample was cooled during transfer from the microreactor to UHV; (b) the sample was cooled to 373 K in the microreactor. The WGS conditions were similar to those of Fig. 1a with a Cs coverage of ~0.27, except the reaction temperature was 523 K.

conditions as noted in Fig. 1a except that the reaction temperature was 523 K. The TDS spectrum (a) is very similar to the TDS spectra in Fig. 1a for Θ_{Cs} = 0.23 and 0.30, except for a slight removal of intensity on the low-temperature side of the TDS peak due to desorption of lower-temperature states during cooling and evacuation starting from this higher reaction temperature. The only difference between the two spectra in Fig. 3 is the appearance of a low-temperature shoulder at 451 K in TDS (b) corresponding to the surface cooled in the reactor. The presence of this lower-temperature desorption state can be explained by the presence of a higher CO_3 : Cs ratio (see below). Although this species desorbs below the reaction temperature of 523 K in UHV, at the CO_2 partial pressures present under reaction conditions, it is likely to have a substantial population.

The CO_2 TDS peak from the Cs-promoted ($\Theta_{Cs} \approx 0.2$) Cu(110) surface after the WGS reaction (at 523 K) showed a shift of about 30 K to lower temperatures as the CO pressure was increased over the range 13 to 190 Torr. The CO_2 TDS peak areas were not noticeably affected, however, and remained fairly constant over all CO pressures. Since the WGS rate is approximately half-order in CO pressure under these conditions (*8*), this shift might be due to either the corresponding increase in CO_2 or H_2 product pressures or directly to the higher CO pressures. This shift in peak temperature was shown not to be caused by the presence of additional CO_2 or H_2 product, because neither the addition of CO_2 to the reaction mixture nor lengthening of the reaction time produced a series of TDS with the same peak temperature trend. Thus, the higher CO flux or coverage at the surface must cause some structural or compositional alteration, resulting in a surface cesium carbonate that decomposes at lower temperatures.

Figure 4 shows the O (1*s*) XPS spectrum of Cu(110) with a cesium coverage of Θ_{Cs} = 0.20 after WGS at 523 K and cooling in the reactor. Also shown are the XPS spectra of that same surface after subsequent rapid anneals in UHV to 548, 698, and 823 K. The spectra clearly show the existence of an oxygen-containing complex formed on Cs/Cu(110) under the WGS reaction conditions, whereas no surface oxygen was present on the postreaction surface without cesium (*8*). For the postreaction XPS peak (a), the O (1*s*) peak position is 531.4 eV BE (binding energy) with a full width at half maximum (FWHM) of 2.8 eV. This binding energy is very similar to the 531.3 eV value (2.4 eV FWHM) found for $Cs \cdot CO_{3,a}$ obtained from dosing CO_2 to the Cs-covered Cu(110) surface in UHV (*25*). The extra width here may be due to the additional presence of other, minority species. Also, the C (1*s*) and Cs ($3d_{5/2}$) peaks were located at 288.9 and 724.5 eV binding energy, respectively, and were very similar to the values for the UHV-dosed $Cs \cdot CO_{3,a}$ of 289.2 and 725.1 eV (*25*). The O (1*s*) binding energy is inconsistent with $Cs \cdot OH_a$ or Cs · Oa, which appear at 530.4–530.8 eV (*30*) and 528.5–529 eV (*30*), respectively. The O (1*s*) and C (1*s*) spectra

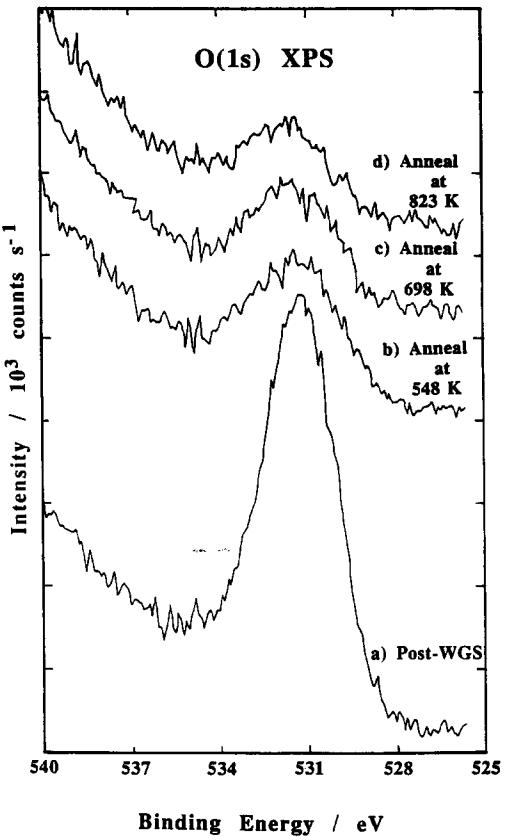

FIG. 4. XPS spectra of carbonate produced during WGS and after thermal treatment. (a) After WGS reaction of 10 Torr H_2O and 26 Torr CO at 523 K for 3 min on Cu(110) precovered with $\Theta_{Cs} = 0.20$. (b–d) After brief annealing at the indicated temperatures.

are also entirely inconsistent with a combination of features from CO_a (*25*) plus O_a (*30*) on Cs-doped Cu(110).

Based on the integration of XPS peaks and atomic sensitivity factors very accurately calibrated on this same spectrometer (*25, 30*), the atomic coverages of cesium, carbon, and oxygen on the post-WGS Cs/Cu(110) surface were 0.20, 0.43, and 1.32 atoms per surface Cu atom, respectively. (These values should be accurate to about 5%.) The stoichiometries are consistent with the soichiometry of a surface carbonate species, $Cs_x \cdot CO_3$, where $x \approx \frac{1}{2}$. The carbonate coverage estimated from these XPS areas is ~0.43 CO_3 units per Cu surface atom, or ~2 CO_3 units per Cs atom. The XPS of a similar Cs/Cu(110) surface taken after WGS reaction but without cooling in the reaction mixture gave ~1.5 CO_3 units per Cs atom, indicating that the working catalyst surface has a CO_3 : Cs ratio somewhere between these two limits. The surface carbonate produced by UHV dosing of CO_2 (22 L at 110 K) to a close-packed monolayer of Cs ($\Theta_{Cs} = 0.48$) on Cu(110) (exemplified by the TDS of Fig. 1b), gave a CO_3/Cs atomic ratio measured by XPS of ~1 (after annealing at 373 K to eliminate all other species such as CO_a and $CO_{2,a}$) (*25*).

After flashing the postreaction surface to 548 K, the C (1*s*) peak disappears, and the O (1*s*) peak area decreases by ~65% (Fig. 4), reasonably consistent with the evolution of CO_2 shown in the TDS of Fig. 1a. This occurs in our model via the reaction

$$Cs \cdot (CO_3)_{2,a} \rightleftharpoons 2CO_2 + Cs \cdot O_a + O_a, \quad (-II')$$

which should give a 67% decrease in the O (1*s*) area if no other oxygen-containing species are present. A larger decrease was seen after decomposition of the UHV-dosed Cs carbonate on Cu(110), but some oxygen was also lost due to diffusion into the bulk (*25*). The O (1*s*) peak position of 531.5 eV after annealing the carbonate to remove CO_2 is different from the results for UHV-dosed carbonate where only adsorbed oxygen and cesium were left on the cesium-covered surface as $Cs \cdot O_a$ (528.6 eV) (*25*). Because of the long acquisition time for XPS (~10 min) and the high background pressure after WGS reaction (10^{-9} to 10^{-8} Torr, mainly H_2O), this difference is possibly due in part to a known reaction of $Cs \cdot O_a$ with background water to produce $Cs \cdot OH_a$ plus OH_a, which appears at ~531 eV binding energy (*30*). This adds to the O (1*s*) signal, and thereby compensates for oxygen lost to the bulk by diffusion (see above). There may also be other minority species present that we cannot identify.

Further annealing to 823 K reduces the width of the O (1*s*) peaks (2.9 eV) and caused

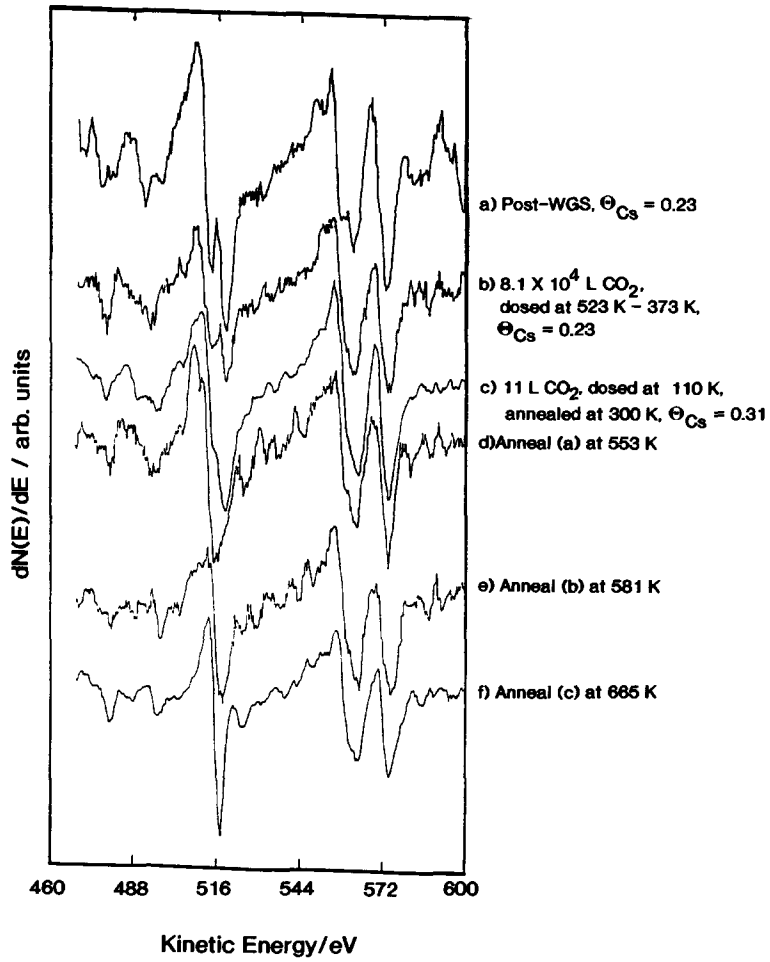

FIG. 5. Comparison of postreaction AES spectra with the spectrum of the surface cesium carbonate produced by dosing in UHV. (a) After WGS reaction of 10 Torr H_2O and 26 Torr CO at 523 K for 3 min on Cu(110) precovered with Θ_{Cs} = 0.23. (b) After dosing 8.1 × 10^4 L CO_2 at 523 K to Cu(110) precovered with Θ_{Cs} = 0.23. (c) After dosing 11 L CO_2 at ~110 K to Cu(110) precovered with Θ_{Cs} = 0.31, and then annealing at 300 K (from (*25*)). (d–f) After annealing (a–c), respectively, at the indicated temperatures.

further shifting to higher binding energy (532.0 eV). Again, water impurity accumulated during data acquisition might complicate this spectrum. However, the general loss of oxygen with increasing annealing temperature is expected (*30*).

Figure 5 shows a comparison of the AES spectra for the Cs/Cu(110) surface ($\Theta_{Cs} \approx$ 0.2) following the WGS reaction and of the surface containing surface Cs carbonate produced by UHV dosing of CO_2 to the Cs/Cu(110) surface at high and low temperatures. Care was taken in these spectra to minimize beam damage, as described previously (*25, 31*). Spectrum 4a was taken after 3 min of WGS reaction using 10 Torr H_2O, 26 Torr CO, 523 K, and cooling in the reactor. The spectrum displays well-defined double minima in the O (KVV) region. The surface that gave spectrum 4b (Fig. 4b) was produced as follows: the clean Cu(110) was first dosed with Θ_{Cs} = 0.23; then it was

exposed to 8.1×10^4 L of CO_2 at 523 K and another 1.7×10^4 L of CO_2 while cooling to 373 K, with an effective CO_2 pressure of 2.25×10^{-4} Torr. Such preparation gave XPS and TDS spectra very similar to those for surface Cs carbonate described above. This dosing procedure also reproduces in AES the double minima as well as most of the features in the fine structure seen in the postreaction spectrum (Fig. 4a). Spectrum 4c (from Ref. (*25*)) was taken after dosing 11 L CO_2 at ~110 K and then annealing the CO_2-dosed surface at 300 K to remove adsorbed CO and weakly adsorbed CO_2, leaving only $Cs \cdot CO_{3,a}$ on the surface. The O (KVV) region shows double minima as in the previous two spectra, but more poorly resolved. Also, the presence of two peaks here is obvious from the large width of the peak, especially from the large peak-to-peak energy separation of 8.2 eV, which is about the same as in the top two spectra. These AES results are further evidence that the cesium carbonate species produced under all three conditions are quite similar.

The spectra 4d, 4e, 4f in Fig. 4 were taken after annealing the surfaces of 4a, 4b, 4c, respectively, in UHV to 553 K or above. Spectrum 4d was taken after annealing the post-WGS surface (4a) to 553 K, which is sufficient to decompose most but possibly not all of the surface carbonate (see Fig. 1). There is a considerable reduction in the width of the O (KVV) peak to a sharp singlet, which indicates that most of the surface is covered with adsorbed oxygen, O_a or $Cs \cdot O_a$. The anneal of the CO_2-dosed surface of spectrum 4b to 581 K produced the surface probed in spectrum 4e, which shows an even sharper O (KVV) peak than 4d because almost all the $Cs_x \cdot CO_{3,a}$ should be decomposed by 581 K. Spectrum 4f followed the 665 K annealing of the surface dosed with CO_2 at 100 K (4c, taken from Ref. (*25*)). The oxygen peak in 4f is the sharpest of the three spectra, 4d–4f, since only $Cs \cdot O_a$ is left on the surface after this treatment (*25*). In general, the surfaces (a, b, and c) containing carbonate show a large peak-to-peak separation of 8.2 to 10.6 eV, whereas after the anneal, the surfaces (d, e, and f) show a much smaller energy separation of ~4.5 eV, more representative of O_a or $Cs \cdot O_a$ (*25, 31*). The smaller differences in width of the O (KVV) peaks between the annealed surfaces (4d–4f) may be related to the O/Cs ratio, which is near unity after low exposure dosing (4c, 4f) (*25*) and ~2 for the post-WGS surface (4a, 4d), or it may be due to the presence of water-related impurities. The decomposition of the post-WGS carbonate was more susceptible to such impurities due to the higher pressure following WGS (Fig. 5d). Such impurities may result in some inequivalent oxygen adatoms that may contribute to the width of the AES peak.

The LEED pattern of the post-reaction Cs/Cu(110) surface for a reaction temperature of 523 K showed only sharp $p(1 \times 1)$ spots with high background intensity. At lower reaction temperatures, such as 473 and 493 K, a streaky (2×1) pattern appeared, but it was not studied in detail. No LEED observations were performed for $Cs \cdot CO_{3,a}$ produced from low exposures of CO_2 such as those used in Fig. 1b (*25*).

3. *Elementary Step Analysis*

a. CO_2/Cs/Cu(110). The Cu(110) surface predosed with $\Theta_{Cs} = 0.17$ was dosed at high temperature (423 K) with high exposures of pure CO_2 (10^3–10^5 L) at 10^{-5} to 10^{-4} Torr. The XPS and TDS measurements after such exposures were consistent with the formation of a surface Cs carbonate, $Cs \cdot CO_{3,a}$, such as that seen previously (*25*) from lower exposures of CO_2 in UHV to cold (110 K) Cs/Cu(110) followed by warming to 300 K. A substantial difference, however, is that much higher CO_2 exposures were needed at 423 K to approach saturation, $\sim 3 \times 10^4$ L, compared to only ~2.3 L at 110 K (*25*). This suggests that the carbonate is formed via a weakly adsorbed CO_2 precursor whose activation energy for desorption is higher than its activation energy to form carbonate. A cesium-stabilized CO_2 adsorption state that

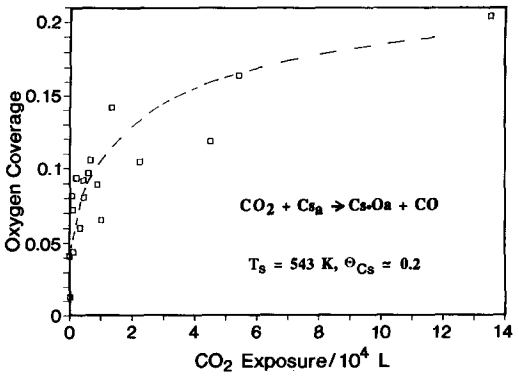

FIG. 6. Coverage of adsorbed oxygen as a function of CO_2 exposure to Cs/Cu(110) at 543 K. This oxygen is produced by the net reaction $Cs_a + CO_2 \rightarrow Cs \cdot O_a + CO$. The Cs precoverage was $0.15 \leq \Theta_{Cs} \leq 0.20$. Coverages were determined by AES.

desorbs in TDS at ~130 K has been previously reported (*25*). Its activation energy for desorption must be around 8.3 ± 0.6 kcal/mol if it desorbs with a preexponential factor of 10^{13}–10^{15} s^{-1}. The activation energy for its reaction to produce carbonate, if this species is indeed the suggested precursor, must then be only about ~5 kcal/mol.

Since adsorbed Cs reacts with CO_2 via

$$2CO_2 + Cs_a \rightarrow Cs \cdot CO_{3,a} + CO \quad \text{(I)}$$

(or via related reactions to produce a higher stoichiometry in the carbonate) and since this carbonate decomposes by about 560 K in TDS via reaction (-II) when Θ_{Cs} is less than ~0.3, then the interaction of CO_2 with Cs/Cu(110) in UHV at temperatures above about 540 K should give the net reaction

$$Cs_a + CO_2 \rightarrow Cs \cdot O_a + CO \quad \text{(III)}$$

(or a related reaction that yields higher stoichiometry in the surface cesium oxide). Figure 6 shows oxygen uptake as a function of CO_2 exposure at 543 K onto Cs predosed Cu(110) via reaction (III), as measured by monitoring the O (KVV) peak-to-peak intensity in AES. Here, the initial Cs coverage was approximately 0.2. The slope of this uptake curve allows us to calculate the CO_2 dissociative adsorption probability on Cs/Cu(110) via the net reaction (III). The resulting initial CO_2 dissociation probability of $\sim 10^{-4}$ at low oxygen coverage is much larger than the CO_2 dissociation probability on Cu(110) in the absence of Cs_a (10^{-10}–10^{-9}) at the same temperature (*26*). The rate of CO_2 dissociation on Cs/Cu(110) decreased to less than ~1% of its initial value when the oxygen coverage grew to a value comparable to the Cs coverage (i.e., at a 1 : 1 ratio of O : Cs). These results suggest that the initial reaction leading to CO_2 dissociation is due to some direct interaction of CO_2 with free Cs_a and that the reactivity for dissociation decreases strongly as each Cs adatom becomes associated with a surface oxygen atom. However, reaction with CO_2 does not stop completely at this 1 : 1 stoichiometry since we were able to push the oxygen coverage achieved in this way up to twice the Cs coverage by dosing with CO_2 at ~100 Torr in the microreactor.

b. $CO_2/O_a/Cs/Cu(110)$. CO_2 was dosed to Cu(110) that was precovered with coadsorbed cesium and oxygen to see whether the surface cesium carbonate could be formed from gaseous CO_2 and $Cs \cdot O_a$. Cesium was adsorbed in UHV first, to a coverage of $\Theta_{Cs} \approx 0.18$. Then after further dosing 2.8 L O_2 to the cesium-dosed Cu(110) surface and heating to 500 K in UHV, surface $Cs \cdot O_a$ is produced with an oxygen coverage of $\Theta_O = \Theta_{Cs} \approx 0.18$. (This $Cs \cdot O_a$ was previously reported to be produced by such a procedure (*30*).) This $Cs \cdot O_a$ was then dosed with increasing exposures of CO_2 to form the adsorbed carbonate. Figure 7 shows the carbonate coverage obtained versus the CO_2 exposure at both 373 and 473 K. The reaction probability is approximately unity at low exposure, but falls by a factor of ~20 by the time the carbonate coverage equals the cesium coverage. In TDS, AES, and XPS, the spectra of the $Cs_x \cdot CO_{3,a}$ produced after such CO_2 exposures to $Cs \cdot O_a$ were very similar to the spectra of the $Cs_x \cdot CO_{3,a}$ produced after dosing just CO_2 (no preadsorbed oxygen) to the Cs/Cu(110) surface at

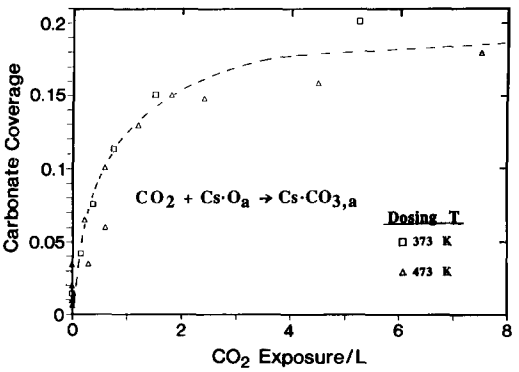

FIG. 7. Carbonate coverage (defined as the number of $CO_{3,a}$ units per Cu surface atom) as a function of CO_2 exposure to an oxygen-precovered Cs/Cu(110) surface. The Cu(110) surface with ~0.18 ML of Cs was exposed to 2.8 L O_2 at 300 K, and then annealed at 583 K to produce $Cs \cdot O_a$ prior to CO_2 dosing. The oxygen and cesium coverages were each then ~0.18. This surface was then exposed to CO_2 under the conditions shown. The carbonate coverages produced in this way were determined from the areas under the CO_2 TDS peaks associated with carbonate decomposition. The absolute carbonate coverages were calibrated by the O (1s) intensity in XPS for a few of the exposures here.

$\sim 10^{-4}$ Torr and 423 K or by dosing CO_2 at 110 K. The results of Figs. 1 and 6 show that

$$Cs_x \cdot CO_{3,a} \rightleftharpoons CO_2 + Cs_x \cdot O_a \quad (-II)$$

is reversible and that the reverse step is also a rapid and viable pathway for carbonate formation, at least up to a stoichiometry of one CO_3 per Cs atom. The combination of Figs. 6 and 7 proves that CO_2 can interact with Cs_a at 523 K to give the reaction $CO_2 + Cs_a \rightarrow CO + Cs \cdot O_a$ with a probability of 10^{-4} per CO_2 collision with the surface, which would be followed very rapidly by the reaction, $CO_2 + Cs \cdot O_a \rightarrow Cs \cdot CO_{3,a}$. Thus, the net probability for CO_2 to produce $Cs \cdot CO_{3,a}$ should be $\sim 10^{-4}$ at a reaction temperature of 523 K and at a Cs coverage of ~0.2. This proves that the Cs_a will be very rapidly converted into the carbonate form under WGS conditions as soon as CO_2 product appears. However, this carbonate can also rapidly decompose (*25*). We consider this formation/decomposition equilibrium in the Discussion. A few, very high exposure points were also taken (not shown in Fig. 7) that increased Θ_{CO_3} to a maximum of ~0.4 (stoichiometry of $x = \frac{1}{2}$ for $Cs_x \cdot CO_{3,a}$) with a reaction probability of $\sim 10^{-5}$–10^{-4} for carbonate formation in the coverage range $\Theta_{CO_3} > 0.2$.

c. Titration of adsorbed oxygen by CO on Cs/Cu(110). Adsorbed oxygen on clean Cu(110) is well known to react with CO gas to produce CO_2 via a Langmuir–Hinshelwood mechanism (*41–43*) involving the step

$$CO_a + O_a \rightarrow CO_2. \quad (IV')$$

This section investigates this same so-called titration reaction on Cs-doped Cu(110). Figure 8 shows the removal of oxygen coadsorbed with $\Theta_{Cs} = 0.17 \pm 0.05$, as a function of CO exposure at surface temperatures of 523 and 573 K. By analogy with the reaction in the absence of Cs_a, this oxygen removal has undoubtedly occurred by the net reaction

$$Cs_x \cdot O_a + CO \rightarrow CO_2 + Cs_{x,a}, \quad (IV)$$

although we have not specifically monitored for CO_2 product here. At these surface temperatures, CO has a short residence time (*44*) and carbonate decomposition is facile (see Figs. 1 and 2); therefore, the only oxy-

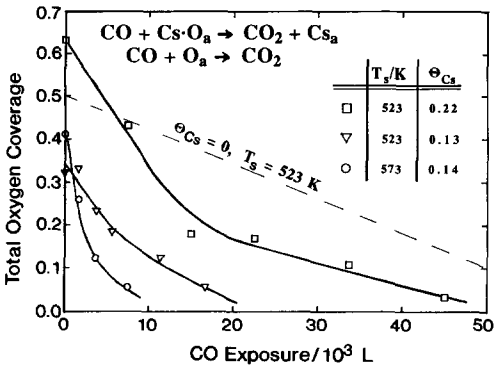

FIG. 8. Titration of adsorbed oxygen by CO on Cs/Cu(110). The Cs-covered surface was exposed to 70 L O_2 and then annealed at 523 K prior to titration reaction. Coverages were determined by XPS. The line for the titration of oxygen from Cu(110) with no Cs_a was taken from Ref. (*43*).

gen-containing surface species at measurable concentrations are oxygen adatoms (O_a or $Cs \cdot O_a$).

In the experiments of Fig. 8, O_2 was dosed at room temperature to a Cu(110) surface with preadsorbed cesium. After O_2 was dosed and heated to reaction temperature, there were two unresolved O (1*s*) peaks in XPS when relatively high oxygen coverages were attained; one was at 530.3 eV, consistent with oxygen adatoms on clean copper (*30*), and the other was at 529.5 eV, assigned previously to "Cs-affected" oxygen adatoms (*30*), which we label $Cs \cdot O_a$. The integrated O (1*s*) areas for the titration denoted by the squares in Fig. 8 indicated an initial total oxygen coverage of $\Theta_O = 0.63$ (O_a plus $Cs \cdot O_a$). The surface was heated to the reaction temperature and then exposed to $\sim 1 \times 10^{-5}$ Torr of CO. The oxygen coverage as a function of CO exposure was then measured from the integrated O (1*s*) XPS peak area. The titration reaction's rate decreases as oxygen is removed, as seen in Fig. 8 by the changing slope. Also, the lower-binding-energy O (1*s*) peak associated with $Cs \cdot O_a$ was titrated first, disappearing below $\Theta_O = 0.18$; subsequently, the higher-binding-energy peak associated with O_a was removed. There was a concomitant partial loss of Cs from the surface as $Cs \cdot O_a$ was removed, consistent with the known fact that pure Cs_a is stable at these reaction temperatures only at lower coverages when oxygen is not present (*30*). The decay in the rate may reflect the weakening of electronic effects with the loss of Cs adatoms.

From the average of the slopes in Fig. 8 above $\Theta_o = 0.18$ at 523 K, the average reaction probability for "Cs-affected" oxygen or $Cs \cdot O_a$ is $\sim 8 \times 10^{-5}$ per collision of CO with the surface. Below $\Theta_o = 0.18$, where the oxygen is present as O_a according to XPS, the reaction probability decreased to $\sim 2 \times 10^{-5}$ per CO collision with the surface. The latter reaction probability is fairly close to the probability reported for the reaction of CO with oxygen adatoms on *clean* Cu(110) at 525 K of $\sim 3 \times 10^{-5}$ per CO collision with the surface (*43*).

The titration of $Cs \cdot O_a$ is obviously much faster than the titration of adsorbed oxygen from clean Cu(110). This may be due to the known Cs-induced increase in the heat of adsorption for CO (*25*). According to the kinetic model reported for the $CO + O_a \rightarrow CO_2$ reaction on clean Cu(110) (*42, 43*), this increase in the heat of adsorption and the consequential lengthening of the CO residence time, together with a known but slight Cs-induced increase in the CO sticking probability (*25*), should produce an increase in the CO reaction probability with oxygen. This increase can apparently overcome any possible increase in the activation energy for the Langmuir–Hinshelwood step brought about by the known stabilization of oxygen adatoms by cesium, $Cs \cdot O_a$ (*30*). The major point here is that oxygen, when coadsorbed with Cs, particularly as $Cs \cdot O_a$, does indeed react with CO to produce CO_2 with a rate that is about four times faster than the same reaction on clean Cu(110) at temperatures where we studied the WGS kinetics. The reaction is, of course, thought to be the final elementary step that leads to CO_2 product in WGS, at least on clean Cu(110) (*8*).

IV. DISCUSSION

Our present TDS, XPS, and AES results indicate that surface carbonate is the major stable species on the Cs-promoted Cu(110) surface following the WGS reaction. The carbonate state corresponding to the 530 K CO_2 peak in postreaction TDS appears for all submonolayer Cs coverages following WGS conditions (see Fig. 1a). For carbonate formed from low exposures (~2–20 L) of CO_2 at 110K, this low temperature TDS state peaks at slightly higher temperatures for the same Cs coverage, and it is found *only* for low Cs coverages ($\Theta_{Cs} < 0.2$) (see Fig. 1). XPS shows that 1.5 to 2 CO_3 units per Cs atom are formed during WGS, compared to only one CO_3 unit per Cs (at

$\Theta_{Cs} = 0.5$) for a 22-L exposure to CO_2 at 110 K (*25*). Therefore, this low-temperature CO_2 TDS peak as well as the even lower temperature peak seen after cooling in the microreactor (Fig. 3) probably reflects a reduction in the stabilization energy induced by the cesium atom when associated with more than one CO_3 unit. The fixed 2.3-L exposure of Fig. 1b might only have been enough to produce a CO_3 : Cs ratio above unity whenever the initial amount of Cs_a was low. By first-order Redhead analysis (*45*) of this 530 K TDS state, the activation energy of carbonate decomposition at 530 K is 30–35 kcal/mol, assuming a prefactor of 10^{12}–10^{14} s^{-1}. The higher-temperature peaks reflect barriers that are 10–30% higher.

The high CO_3 : Cs ratios in this surface complex near the optimum Cs coverage clearly indicate that the carbonate ligands are bonding both to Cu and to the Cs ions. Thus, one can also think of this species as adsorbed carbonate stabilized by Cs. Apparently, at least two carbonates can thus surround a single Cs adatom. Adsorbed carbonate is formed from $CO_2 + O_a$ on Ag(110) even in the absence of alkali (*51*), although this reaction does not occur on Cu(110) without alkali (*52*).

The TDS results shown in Fig. 1a indicate that the form of the post-WGS carbonate is quite similar for all nonzero cesium coverages below about 0.25. The growth of the 530 K CO_2 TDS peak area parallels the increase of Θ_{Cs} (Fig. 2) and the concomitant increase in reaction rate up to $\Theta_{Cs} = 0.25$, where the WGS rate is at a maximum. Above $\Theta_{Cs} = 0.25$, the carbonate coverage increases by the addition of more stable carbonate species that desorb at higher temperatures in TDS (see Fig. 1a), which more closely resemble bulk Cs_2CO_3 (*25*). Here, the reaction rate decreases, obviously because free Cu surface sites are also somehow necessary for the reaction. It is interesting to note that the maximum promotional effect on the WGS rate occurs at the Cs coverage that gives the minimum in the Cs-induced work function change (for pure Cs_a) (*25*). This is the coverage where Cs_a itself also begins to suddenly look more bulk-like (i.e., more metallic rather than ionic) (*25*). The appearance of higher-temperature carbonate states in TDS, the decline in WGS rate, and the more bulk-like character of the as-dosed Cs all seem to correlate. On clean Cu(110), a $CO_{3,a}$ species is not observed after the WGS reaction or after dosing CO_2 to clean or to oxygen-covered Cu(110) (*25, 26*). This suggests that the carbonate associated with the 530 K CO_2 TDS peak is a contributing factor in the Cs promotion of the WGS reaction, and that the rate becomes inhibited by the increase in the steady-state coverage of more stable, bulk-like carbonate species.

Since CO_2 alone easily produces the surface carbonate on the Cs/Cu(110) surface (see above), product CO_2 can produce $Cs_x \cdot CO_{3,a}$ under reaction conditions. The small differences in the CO_2 TDS and in the XPS after carbonate decomposition under WGS conditions versus UHV dosing of CO_2 indicate that the presence of other adsorbed species affect the nature of the carbonate thus formed, although stoichiometric differences alone resulting from the larger exposures during WGS may explain most of these changes.

This surface Cs carbonate can also be formed from $Cs \cdot O_a$ by exposure to CO_2 gas, as shown in Fig. 7. Thus, one must consider a dynamic equilibrium of the form

$$CO_2 + Cs_x \cdot O_a \rightleftharpoons Cs_x \cdot CO_{3,a}, \quad \text{(II)}$$

where x is a fraction apparently close to one-half under reaction conditions. The forward process proceeds at 550 K with an initial reaction probability (p_{CO_2}) per CO_2 collision with the surface, which is close to unity when the $Cs_x \cdot O_a$ concentration is still high (Fig. 7). Let us assume that this rate is first-order in the $Cs_x \cdot O_a$ concentration, which is approximately true for the shape of Fig. 7. The reverse (decomposition) process occurs as a quasi-first-order process with an activation energy (E_a) of about 32 kcal/mol and a prefactor (υ) of $\sim 10^{13}$ s^{-1}. These rate con-

stants imply that at equilibrium, in the absence of other complicating reactions or adsorbed species, the surface cesium "carbonate" and "oxide" will be in the approximate concentration ratio

$$\Theta_{Cs_x(CO_3)_{n,a}}/\Theta_{Cs_xO_a} = P_{CO_2} \cdot f_{CO_2} \cdot p_{CO_2}/k_{decomp}, \quad (1)$$

where f_{CO_2} is the collision frequency of CO_2 with the surface per unit pressure ($\sim 2.3 \times 10^{20}$ cm^{-2} s^{-1} Torr^{-1} at 550 K), and $k_{decomp} = \upsilon \cdot e^{E_a/RT}$ (~ 2.0 s^{-1} at 550 K). At 10 Torr H_2O, 26 Torr CO, and 550 K, after our typical reaction times, the CO_2 product partial pressure in the microreactor was about 0.2 Torr. At this CO_2 pressure and 550 K, the carbonate : oxide ratio predicted for this equilibrium using these constants is $\sim 1.5 \times 10^4$. Thus, our observed kinetics imply that the equilibrium (II) lies far to the right, that the free $Cs_x \cdot O_a$ coverage will be very low, and that the major form of the Cs will be that of the carbonate. This is consistent with our postreaction surface analysis.

Of course, one must consider that CO, H_2, and H_2O also compete for the surface $Cs_x \cdot O_a$ via the known reactions

$$Cs_x \cdot O_a + CO_a \rightarrow CO_2 + Cs_a, \quad \text{(IV)}$$

$$Cs_x \cdot O_a + H_2O_a \rightarrow CsOH_a + OH_a \quad (30), \quad \text{(V)}$$

and

$$Cs_x \cdot O_a + H_2 \rightarrow Cs_a + H_2O \quad (38), \quad \text{(VI)}$$

so the free $Cs_x \cdot O_a$ coverage should be even lower than predicted above.

Adsorbed oxygen is known to react with H_2O to produce adsorbed surface hydroxyls, OH_a, on clean and Cs-promoted Cu(110) (*30*). The hydroxyls disproportionate to release H_2O and surface oxygen at about 290 K on clean Cu(110) (*29*) and at about 340–390 K on Cs-doped Cu (*30*). Thus, the cesium stabilizes surface hydroxyls. An extremely stable hydroxyl, attributed to adsorbed cesium hydroxide, $CsOH_a$, is also formed on Cs/Cu(110) when Θ_{Cs} exceeds about 0.25 (*30*). This species has a desorption energy of ~30 kcal/mol (*30*), and is stable to about 510 K in UHV. This species, however, was not seen at high concentrations in post-WGS analysis at the optimum Cs coverage. In addition, TDS experiments have also shown that H_a is more stable (*30*) when Cs_a is present. Although H_2O_a is certainly also stabilized by Cs_a (*30, 31*), it is not stabilized nearly as much as the combination of OH_a and H_a are stabilized, based on a qualitative comparison of TDS peak temperatures with and without Cs_a addition (*30*). From a simple application of the linear Brønsted relationships, one would expect the barrier for the process $H_2O_a \rightarrow OH_a + H_a$ to decrease if the $OH_a + H_a$ is stabilized more than H_2O_a by Cs. Thus, one would certainly expect surface Cs to facilitate H_2O_a dissociation on Cu(110). Since water dissociation is the rate-determining step on clean Cu(110), this indirect electronic effect alone may explain the promotional role of Cs in WGS. Since $Cs_x \cdot CO_{3,a}$ is the dominant form of Cs under reaction conditions, however, it would be more meaningful to make this comparison in stabilities with $Cs_x \cdot CO_{3,a}$ rather than Cs_a as a surface additive.

The electronic effects of "carbonate-stabilized" cesium upon other adsorbates should be at least qualitatively similar to the effects of Cs_a alone, since both species should cause a work function decrease relative to clean Cu (*46*). Since Cs_a alone should decrease the barrier for water dissociation on Cu (see above) and thereby increase its rate, one should also expect the surface Cs carbonate to do the same. Therefore, the increase in activity brought about by cesium addition may be simply due to an acceleration in the rate of water dissociation due to electronic effects of $Cs \cdot CO_{3,a}$ on the activation barrier. If this effect is strong enough, it would accelerate water dissociation to such an extent that it is no longer rate-limiting. This would be consistent with

the decrease in reaction order with respect to H_2O.

Cesium also has an electronic effect on the adsorption of CO and the interaction of CO with adsorbed oxygen. Adsorbed CO is stabilized at low coverages of cesium ($\Theta_{Cs} \leq 0.25$), increasing its TDS desorption temperature by ~15% (*25*). Adsorbed oxygen is also stabilized by cesium (*30*), yet the reaction of CO with O_a proceeds with higher probability on Cs-promoted Cu(110) (Fig. 8).

On clean Cu(110), the following "surface redox" or "oxygen adatom" mechanism was shown to be consistent with the measured WGS kinetics and with the kinetics of the elementary steps as described in Ref. (*8*):

$$H_2O_g \rightleftharpoons H_2O_a, \quad \text{(i)}$$

$$H_2O_a \rightleftharpoons OH_a + H_a, \quad \text{(ii)}$$

$$OH_a \rightleftharpoons O_a + H_a, \quad \text{(iii)}$$

$$2H_a \rightleftharpoons H_{2,g}, \quad \text{(iv)}$$

$$CO_g \rightleftharpoons CO_a, \quad \text{(v)}$$

$$CO_a + O_a \rightleftharpoons CO_{2,g}. \quad \text{(vi)}$$

Step (iii) can also be written as a "water-catalyzed" step, whose kinetics were shown to be consistent with the rates obtained on clean Cu(110) for the WGS and for Step (iii) [8]:

$$H_2O_g \rightleftharpoons H_2O_a, \quad \text{(i)}$$

$$H_2O_a \rightleftharpoons OH_a + H_a, \quad \text{(ii)}$$

$$2OH_a \rightleftharpoons O_a + H_2O_a, \quad \text{(viii)}$$

$$H_2O_a \rightleftharpoons H_2O_g, \quad \text{(-i)}$$

$$\text{Net:} \quad OH_a \rightleftharpoons O_a + H_a. \quad \text{(iii)}$$

Analysis of the WGS reaction kinetics on clean Cu(110) has shown that the dissociation of H_2O (Step (ii)) is the RDS over all reactant pressures tested (*8*).

Kinetic studies of the WGS reaction have shown that the apparent activation barrier for the WGS over clean and over Cs-covered Cu(110) (*8*) and Cu(111) (*7*) are nearly the same, although slightly larger in both cases for the Cs-doped surfaces. Reaction orders, however, differ greatly between the clean Cu(110) surface and the Cs-promoted Cu(110) surface at low CO pressures (<100 Torr CO). Namely, whereas the reaction is first-order in H_2O and zero-order in CO on clean Cu(110), the order in H_2O is nearly zero and that in CO is about 0.5 on the optimally promoted surface. This proves that water dissociation is no longer the clearly rate-determining step on the Cs-promoted Cu(110) surface, at least at low CO pressures, but that the reaction rate must be somehow partially limited by CO adsorption or reaction. It must be coincidental that this change occurs with only a slight increase in the apparent activation energy. The noninteger orders and their changes with reaction conditions show that there is no clear, single rate-determining step on the Cs-promoted Cu(110) surface. The WGS on Cs-promoted Cu(111) also shows only a small (~1 kcal/mol) increase in the apparent activation energy from the clean Cu(111) surface (*7*). On Cs/Cu(111), however, the rate dependence on H_2O pressure remained close to unity at 612 K and 26 Torr CO, as it was on the clean Cu(111) surface (the CO pressure dependence was not measured (*7*)). Thus, it is unlikely that the rate-determining step changes upon Cs doping of Cu(111), although the rate increases 15-fold (*7*). At 612 K, the rate of WGS on optimally promoted Cs/Cu(111) and that on optimally promoted Cs/Cu(110) are about the same on a per unit area basis; however, the apparent activation energies are quite different (20 kcal/mol versus 11 kcal/mol, respectively).

We assume here that a mechanism similar to the "surface redox" mechanism for WGS on clean Cu(110) is also giving rise to WGS on Cs-promoted Cu(110). In this case, however, we must remember that all adsorbate species may be electronically affected by surface Cs (or $Cs_x \cdot CO_{3,a}$). The magnitude of this electronic effect may also depend on their lateral distance from the Cs adatoms. In addition, reactions (IV), (V), and (VI)

presented above and their reverses must also be considered in the mechanism on Cs-promoted Cu(110).

The surface-redox mechanism favored for the WGS on clean Cu(110) does not include a carbonate species, since $CO_{3,a}$ is not formed on clean Cu(110) even under WGS conditions (*8*). On Cs-promoted Cu(110), where the surface carbonate species is observed after WGS, the apparent activation energy of WGS of 11 kcal/mol (*8*) is very different from the 32 kcal/mol (or larger) activation energy of $Cs \cdot CO_{3,a}$ decomposition. If the "surface redox" mechanism is an accurate description of WGS on Cs/Cu(110), then the surface carbonate formation and decomposition reactions are just side reactions to WGS, which nevertheless maintain the proper ratio of $Cs_x \cdot CO_{3,a}$: $Cs \cdot O_a$. During the titration of adsorbed oxygen by CO, cesium is desorbed when the stabilizing influence of the adsorbed oxygen is removed. As seen in Fig. 1, there is no Cs desorption until the carbonate has decomposed, whereas Cs_a alone desorbs below 500 K (*25*). This proves that the carbonate form stabilizes the Cs layer against desorption, which is necessary to keep it on the surface under WGS conditions.

The high order in CO pressure (~0.5) is consistent with a change in the RDS from water dissociation to the titration of $Cs \cdot O_a$ by CO. If this step completely controlled the WGS rate, a first-order dependence in the WGS rate upon CO coverage would be expected at low CO pressures. At higher CO pressures, the pressure dependence could be somewhat less than first-order as observed here (*8*) because the CO adsorption isotherm (in the presence of Cs) is just beginning to roll over toward saturation, or because this step is not completely rate-limiting.

The WGS reaction rate could be positive order in CO pressure upon Cs addition because CO_2 and H_2O now compete effectively with CO for the available surface oxygen ($Cs \cdot O_a$), where Cs is predominately in the form of carbonate in the dynamic competition:

$$Cs \cdot O_a + CO_2 \rightleftharpoons Cs \cdot CO_{3,a}, \quad \text{(II)}$$

$$Cs \cdot O_a + CO \rightarrow CO_{2,g} + Cs_a, \quad \text{(IV)}$$

$$Cs \cdot O_a + H_2O_a \rightleftharpoons CsOH_a + OH_a. \quad \text{(V)}$$

Consistent with this concept is our observation that the WGS rate over Cs/Cu(110) decreased when CO_2 was added at high concentrations to the reactant feed. This would be expected because of the resulting decrease in the steady-state $Cs \cdot O_a$ concentration. At 523 K, the WGS rate for 10 Torr H_2O and 26 Torr CO is $\sim 5.5 \times 10^{14}$ cm^{-2} s^{-1} with $\Theta_{Cs} = 0.25$. Since the rate of the product-producing Step (IV) equals the WGS rate, this corresponds to a reaction probability of 7.3×10^{-8} per collision of CO with the surface. This value is more than 1000 times smaller than the reaction probability for Step (IV) alone on Cs/Cu(110), when oxygen coverages are a substantial fraction of a monolayer. The much lower probability under WGS conditions means that the surface oxygen coverage ($Cs \cdot O_a$ and O_a) is very low ($\sim 10^{-3}$). The rest of the oxygen is bound up as carbonate and hydroxyl, and its release (by the reverse of steps (II) and (V)) may be partially limiting the rate. The dissociation of water, on the other hand, is definitely *not* the sole rate-determining step for WGS on cesium-promoted Cu(110), except at high CO pressures, since the rate is otherwise nearly zero-order in P_{H_2O}. The low order in H_2O is also partially caused by the competition from H_2O for surface $Cs_x \cdot O_a$ mentioned above.

Surface carbonate has also been identified by NMR and XPS data on the surface of a Cs-promoted precipitated copper catalyst after its use under methanol synthesis conditions (~5 atm., 1:2 CO to H_2 (*47*)). The function proposed in that study for the alkali carbonate was to stabilize Cu^+ (*5, 6, 47*), in accord with similar proposals regarding the role of ZnO supports in Cu/ZnO methanol synthesis catalysts (*48*). A significant coverage of carbonate-stabilized Cu^+ is not a prerequisite for the WGS reaction, however.

The WGS reaction, possibly unlike methanol synthesis, has a significant rate over unpromoted, unsupported, bare copper at very low surface oxygen coverages (*7, 8*). An alternative role for the carbonate as a WGS promoter is the stabilization of the Cs adlayer, as suggested here, and the concomitant electronic effects afforded by this Cs carbonate. It has been proposed that methanol synthesis occurs via hydrogenation of CO_2 (*10, 49*), which is produced by WGS from the CO in the feedstream. Thus, the promotion of methanol synthesis by Cs could occur because of the acceleration of the WGS rate. Interestingly, methanol synthesis is not promoted by cesium when sizeable levels of CO_2 are added to the feedstream, but it is promoted by cesium with pure CO plus H_2 feed and only tiny CO_2 levels (*2*). Perhaps this occurs because the WGS rate is fast enough to resupply CO_2 to keep up with the methanol synthesis rate when operating under conditions where there are high levels of CO_2 (and H_2O), but the WGS rate is not fast enough at low CO_2 (and H_2O) levels. Since cesium accelerates the WGS rate, it may aid in the latter case only.

Some surface analysis has also been performed on the Cs-doped Cu(111) surface after the WGS reaction (*7*). In that study, the reaction was performed at 612 K and the sample was cooled in the reaction mixture to 465 K before transfer to UHV. The Cs ($3d_{5/2}$) peak was seen at 725.1 eV, exactly the same value as seen for UHV-dosed Cs carbonate on Cu(110) (*25*). The O (1*s*) peak was at 531.0 eV (FWHM = 2.8 eV), compared to 531.3 eV (FWHM = 2.4 eV) for $Cs \cdot CO_{3,a}$ prepared under UHV on Cu(110) (*25*). The O (KVV) AES peak also showed a double minimum and a large peak-to-peak energy separation (~9 eV), characteristic of the surface cesium carbonate on Cu(110) (see above). These similarities indicate that the major form of Cs on the postreaction Cu(111) surface is also a surface Cs carbonate, as on Cu(110). In that earlier work on Cu(111), the surface species was postulated to be a surface Cs oxide or hydroxide. The carbon signals in XPS and AES were overlooked in that study because of their small size (only about 10% of the respective signals for oxygen). However, as we show here, the small size of the carbon XPS and AES signals is consistent with carbonate stoichiometry (C : O = 1 : 3), since the XPS and AES sensitivity factors for carbon are only about one-third of those for oxygen.

ACKNOWLEDGMENTS

The authors thank the Department of Energy, Office of Basic Energy Sciences, Division of Chemical Sciences, for funding of this research. C.T.C. acknowledges support from a Camille and Henry Dreyfus Foundation Teacher/Scholar Award.

REFERENCES

1. Bonzel, H. P., *Surf. Sci. Rep.* **8,** 43 (1987).
2. Verdage, G. A., Himelfarb, P. B., Simmons, G. W., and Klier, K., *in* "Solid State Chemistry in Catalysis," ACS Symposium Series 279, pp. 295–312. Am. Chem. Soc., Washington DC, 1985.
3. Klier, K., Young, C. W., and Nunan, J. G., *Ind. Eng. Fundam.* **25,** 36 (1986).
4. Nunan, J. G., Klier, K., Young, C. W., Himelfarb, P. B., and Herman, R. G., *J. Chem. Soc. Commun.*, 193, (1986).
5. Sheffer, G. R., and King, T. S., *J. Catal.* **115,** 376 (1989).
6. Sheffer, G. R., and King, T. S., *J. Catal.* **116,** 488 (1989).
7. Campbell, C. T., and Koel, B. E., *Surf. Sci.* **186,** 393 (1987).
8. Nakamura, J., Campbell, J. M., and Campbell, C. T., *J. Chem. Soc. Faraday Trans. 1* **86,** 2725 (1990).
9. Campbell, C. T., and Daube, K. A., *J. Catal.* **104,** 109 (1987).
10. Chinchen, G. C., Spencer, M. S., Waugh, K. C., and Whan, D. A., *J. Chem. Soc. Faraday Trans. 1* **83,** 2193 (1987).
11. Newsome, D. S., *Catal. Rev.-Sci.* **21,** 275 (1980).
12. van Herwijnen, T., and deJong, W. A., *J. Catal.* **63,** 83 (1980).
13. Salmi, T., and Hakkarainen, R., *Appl. Catal.* **49,** 285 (1989).
14. Fiolitakis, E., and Hofman, H., *J. Catal.* **80,** 328 (1983).
15. Kuijpers, E. G. M., Tjepkema, R. B., van der Wal, W. J. J., Mesters, C. M. A. M., Spronck, S. F. G. M., and Geus, J. W., *Appl. Catal.* **25,** 139 (1986).
16. Hadden, R. A., Vandervell, H. D., Waugh, K. C., and Webb, G., *in* "Proceedings, 9th International

Congress on Catalysis, Calgary, 1988" (M. J. Phillips and M. Ternan, Eds.), Vol. 4, p. 1853. Chem. Institute of Canada, Ottawa, 1988.
17. Ovesen, C. V., Stoltze, P., Nørskov, J. K., and Campbell, C. T., *J. Catal.* **134,** 445 (1992).
18. Horn, K., Hussain, M., and Pritchard, J., *Surf. Sci.* **63,** 244 (1977).
19. Spitzer, A., and Lüth, H., *Surf. Sci.* **102,** 29 (1981).
20. Woodruff, D. P., Hayden, B. E., Prince, K., and Bradshaw, A. M., *Surf. Sci.* **123,** 397 (1982).
21. Rogozik, J., Scheidt, H., Dose, V., K. C. Prince, and Bradshaw, A. M., *Surf. Sci.* **145,** L481 (1984).
22. Gumhalter, B., *Surf. Sci.* **157,** L355 (1985).
23. Harendt, C., Goschnick, J., and Hirschwald, W., *Surf. Sci.* **152/153,** 453 (1985).
24. Lackey, D., Surman, M. Jacobs, S., Grider, D., and King, D. A., *Surf. Sci.* **152/153,** 513 (1985).
25. Rodriguez, J. A., Clendening, W. D., and Campbell, C. T., *J. Phys. Chem.* **93,** 5238 (1989).
26. Nakamura, J., Rodriguez, J. A., and Campbell, C. T., *J. Phys.: Condens. Matter* **1,** SB149 (1989).
27. Spitzer, A., and Lüth, H., *Surf. Sci.* **120,** 376 (1982).
28. Spitzer, A., and Lüth, H., *Surf. Sci.* **160,** 353 (1985).
29. Bange, K., Grider, D. E., Madey, T. E., and Sass, J. K., *Surf. Sci.* **137,** 38 (1984).
30. Clendening, W. D., Rodriguez, J. A., Campbell, J. M., and Campbell, C. T., *Surf. Sci.* **216,** 429 (1989).
31. Lackey, D., Schott, J., Straehler, B., and Sass, J. K., *J. Phys. Chem.* **91,** 1365 (1989).
32. Alexander, C. S., and Pritchard, J., *J. Chem. Soc. Faraday Trans. 1* **68,** 202 (1972).
33. Balooch, M., Cardillo, M. J., Miller, D. R., and Stickney, R. E., *Surf. Sci.* **46,** 358 (1974).
34. Rieder, K. H., and Stocker, W., *Phys. Rev. Lett.* **57,** 2548 (1986).
35. Anger, G., Winkler, A., and Rendulic, K. D., *Surf. Sci.* **220,** 1 (1989).
36. (a) Hayden, B. E., and Lamont, C. L. A., *Chem. Phys. Lett.* **160,** 331 (1989); (b) *Phys. Rev. Lett.* **63,** 1823 (1989).
37. Campbell, J. M., and Campbell, C. T., *Surf. Sci.* **259,** 1, 1991.
38. Ernst, K.-H., Domagala, M. E., Campbell, C. T., and Moretti, G., *Surf. Sci.* **259,** 18, 1991.
39. Fan, W. C., and Ignatiev, A., *Phys. Rev. B* **38,** 366 (1988).
40. Kimmel, G. A., Goodstein, D. M., and Cooper, B. H., *J. Vac. Sci. Technol. A* **7,** 2186 (1989).
41. Ertl, G., *Surf. Sci.* **7,** 309 (1967).
42. Domagala, M., and Campbell, C. T., *Catal. Lett.* **9,** 65 (1991).
43. Habraken, F. H. M. P., Bootsma, G. A., Hofman, P., Hachicha, S., and Bradshaw, A. M., *Surf. Sci.* **88,** 285 (1979).
44. This can be easily shown using the known desorption energy for CO on clean (*18, 23*) or Cs-doped (*25*) Cu(110) (below one-half monolayer).
45. Redhead, P. A., *Vacuum* **12,** 203 (1962).
46. This conclusion is based on our knowledge of many coadsorbate systems involving alkalis on transition metals, all of which have lower work functions than the clean metal.
47. Chu, P. J., Gerstein, B. C., Sheffer, G. R., and King, T. S., *J. Catal.* **115,** 194 (1989).
48. Klier, K., *in* "Advances in Catalysis" (D. D. Eley, H. Pines, and P. B. Weisz, Eds.), Vol. 31, p. 243. Academic Press, San Diego, 1982.
49. Chinchen, G. C., Denny, P. J., Parker, D. G., Spencer, M. S., and Whan, D. A., *Appl. Catal.* **30,** 333 (1987).
50. Henn, F. C., Rodriguez, J. A., and Campbell, C. T., *Surf. Sci.* **236,** 282 (1990).
51. Barteau, M. A., and Madix, R. J., *J. Electron Spectrosc. Relat. Phenom.* **31,** 101 (1983).
52. Nakamura, J., Rodriguez, J. A., and Campbell, C. T., *J. Phys.: Condens. Matter* **1,** SB149 (1989).